Proceedings of the International Symposium on
Thermal Effects in Gas flows In Microscale
October 24-25, 2019 – Ettlingen, Germany

ISTEGIM 2019:285411

SPECTRAL ANALYSIS FOR TUNING THE SLUG FLOWS IN MICROCHANNELS

Maide Bucolo, Salvina Gagliano,
University of Catania DIEEI Catania, Italy
maide.bucolo@unict.it, salvina.gagliano@unict.it

KEY WORDS

Experimental study, Optical signals, non-invasive monitoring, Air-Water flows, velocity in microchannel

ABSTRACT

Standard 3D optical velocity measurements in micro-channels is based on Particle Image Velocimetry (PIV), bulky and costly equipment are necessary to run this analysis. A challenge in this context is the development of velocity detection systems based on optical signals monitoring being non-invasive and suitable for on-chip integration. In this works the attention has been focused on slug flows obtained by the interaction of two immiscible fluids {air and water} in micro-channels (slug flows). An optical-based approach, previously used by the authors, based on the optical signal's acquisition and analysis was extend in a more general framework. The spectral analysis of the optical signals acquired in three different experimental sets was used to investigate the slugs' velocity as an indirect measure of the slugs' frequency passage in a micro-channel test section. The potential of the proposed method was evinced by the possibility to capture, distinctively, the variation in the duration of the water and air slugs running in the microchannel interlaced. Finally the attention was focused in their different behaviors correlated to different input flow rates conditions.

1. INTRODUCTION

The slug flow is common in many bio-chemical processes and its modelling and control is one of the main open issue in the construction of highly complex microsystems [2]. Generally, the models of a multi-phase microfluidics system, in which more fluids and micro-particles interact in a micro-channels network, are obtained by Computational Fluid Dynamics (CFD) [1]-[18]. Even so, the complexity of CFD, due to the high computation level and the not accessible analytical solution, cannot make them suitable for on-chip applications. Otherwise the data-driven models [3]-[6] obtained by optical processes monitoring [9] can represents a good alternative being non-invasive, offering an easy integration of optical sensors with the micro-fluidic chips [8]-[13] and, in future development, the possibility of being even embedded in a chip [4]. Advantages can be also envisaged for SoC applications due to the simplicity of managing optical signals, as it is proved by a wide literature on flow classification in micro-channels using optical signals [10]-[11]. In our recent works the optical signals have been used to characterize the flow nonlinearity [14] and to define parameters in order to classify the slug flow inside the micro-channel [5] for online control application [7].

The challenge in this work is the development of velocity detection systems non-invasive and suitable for on-chip integration, avoiding bulky and costly equipment as the standard 3D optical velocity measurements based on Particle Image Velocimetry [16]-[17].

In this works the attention has been focused on slug flows obtained by the interaction of two immiscible fluids {air and water} in micro-channels (slug flows). An optical-based approach, previously used by the authors for the optical signal's acquisition and analysis, was extend in a more general framework. The

Proceedings of the International Symposium on
Thermal Effects in Gas flows In Microscale
October 24-25, 2019 – Ettlingen, Germany

spectral analysis of the optical signals acquired in three different experimental sets was used to investigate the slugs' velocity as an indirect measure of the slugs' frequency passage in a micro-channel test section. The potential of the proposed method was evinced by the possibility to capture, distinctively, the variation in the duration of the water and air slugs running in the microchannel interlaced. Finally the attention was focused in their different behaviors correlated to different input flow rates conditions.

2. MATERIAL AND METHODS

Three experimental campaigns were realized. In all the experiments considered, a continuous slugs flow was generated by pumping de-ionized water and air at the Y-junction of a serpentine micro-channel in Cyclic olefin copolymer (COC) with a square section and positioned horizontally. The side of the micro-channel is 320 μm. Two neMESYS syringe pumps were connected to the two channel inlets. In the experimental set-1 (labelled as *exp-set-1*) nine experiments were carried out constant where equal flow rates of water (F_w) and air (F_a) were imposed $F \in \{0.1, 0.2, 0.3, 0.4, 0.5, 0.6, 0.7, 0.8, 0.9\}$ ml/min. The flow chart of the experimental set-up is shown in Fig.1(a). The process was monitored in a position after three bends from the Y-junction, see the insert in Fig.1(b).

The optical setup consists in the simultaneous acquisition (sample rate of 2 kHz) of the light intensity variations by a couple of photodiodes placed at a distance of 10 mm. The process was also monitored by CCD to have a process visual inspection. A detailed description of the experimental set-up and the signals pre-processing is given in [5].

The trends of the signals acquired by the two photodiodes {*ph1*, *ph2*} for F=0.2 ml/min are shown in Fig.1(b) As discussed widely in [5], the signal acquired by the photodiode was correlated with the video acquired by the CCD-camera to give a physical interpretation of the signal. In particular, the top level represents the water presence in the channel, while the lower level the air slug passage. The two lowest peaks reveal the slugs fronts and rears. During the slugs passage the intensity of the light signal decreases suddenly due to the difference between the refraction index of COC (N_{COC}=1.5) and air (N_{air}=1), so the air slug contour becomes darker than the inside of the slug and the chip wall. This effect is less evident during the water passage being the water refraction index (N_{water}=1.3) closer to the one of the COC. Thanks to this phenomenon it is possible to distinguish clearly the air slug passage in the optical signals.

In Fig. 2(a) the trends of the raw optical signals are plotted in a time window of 2 s for the experiments $F \in \{0.2, 0.4, 0.6, 0.9\}$ ml/min and 0.5 s for the experiment F=0.9 ml/min.

It is evident that, nevertheless the process nonlinearity do not allow to have a regular passage of the slugs, a clear change in the slug flow patterns can be detect: from long water slugs interlaced with air slugs one after another (F=0.1-0.2 ml/min), to water slugs followed by a train of smaller water/air passages (F=0.3-0.8 ml/min), and finally only a train of smaller air/water slug (F=0.9 ml/min). A slower dynamics can be generally correlated to the passage of long water slug for $F \in [0.1,…,0.8]$, and a fast dynamics associated to trains of smaller water/air slugs of the same length for F=0.9.

For establish the frequency of the slug flow passage two approaches previously used by the authors based on the optical signal's analysis were implemented and compared. The first is based on the spectral analysis used in [5] and the second is based on the dual-slit methodology presented in [12]. The data were acquired for 20 s and a time window of 10 s were used for the analysis, excluding the first and last 5s.

The procedure for the flow characterization in frequency domain was implemented by computing the spectrum of optical signal (*ph2*) for each experiment. The mean frequency of the slugs passage was extracted by the peak detection in the spectrum. The profile of the spectrum was approximated with a Gaussian model. In previous works, this procedure was used for the slug flows classification [5] and for the real-time feed-forward control of the mean frequency of the slugs' passage in micro-channels [7]. In both cases the attention was focused in one dominant peak.

As shown in Fig.2(b), due to the difference in the fluids physical properties, even using the same input flow-rates, two peaks can be detected in spectral analysis. These two dominant frequencies are correlated at the different duration of the passages of water slugs, longer, and air slugs, smaller. In Fig. 2(b) the spectrum of the optical signal for the experiments $F \in \{0.2, 0.4, 0.6, 0.9\}$ ml/min are shown. When the input strength is

A Marie-Curie-ITN
within H2020

Proceedings of the International Symposium on
Thermal Effects in Gas flows In Microscale
October 24-25, 2019 – Ettlingen, Germany

enough strong the flow pattern converges to the behavior of the experiment F=0.9 ml/min, a sequence of water/air slugs of almost the same length (see Fig.2a), so only one dominant peak can be detected in its spectrum.

The procedure for the flow characterization in the time domain was implemented by computing the cross-correlation between the optical signals {*ph1*, *ph2*} for each experiment. The peak detected in the cross-correlation is representative of the time delay of the two signals and can be correlated with the time need to the slug to move from one investigation area to the second. Being known the distance between the two photodiodes positions is possible to establish the slug passage velocity.

In Fig. 2(b) the cross-correlation functions obtained for the experiments F∈{0.2, 0.4, 0.6, 0.9} ml/min are shown. The cross-correlation functions are plotted versus the samples in a time window of 0.1 s (200 samples) for F=0.2 ml/min and 0.05 s (100 sample) for F∈{0.4, 0.6, 0.9}. A sharp peak can be always detected. As expected the increase of the input flow rate leads to a time delay reduction. For the experiment F=0.9 ml/min the characteristic of the flow pattern, as fast train of air and water slugs, is reflected in the oscillatory trend of the cross-correlation.

The other two experimental campaigns {*expe-set-2*, *expe-set-3*} were performed using the same experimental set-up but varying the input flow rate conditions in unbalanced conditions. In both cases, the water input flow rate was varied F_w∈{0.1, 0.2, 0.3, 0.4} ml/min. In the *expe-set-2* the air input flow rate was set to Fa∈{0.15, 0.3, 0.45, 0.6} ml/min having Fa=1.5* Fw. In the *expe-set-3* the air input flow rate was set to Fa∈{0.2, 0.4, 0.6, 0.8} ml/min having Fa=2* Fw. Based on the input flow rates established for the three experimental campaigns {*expe-set-1*, *expe-set-2*, *expe-set-3*} the Air Fraction (AF) was respectively AF∈ {0.5, 0.6, 0.67}.
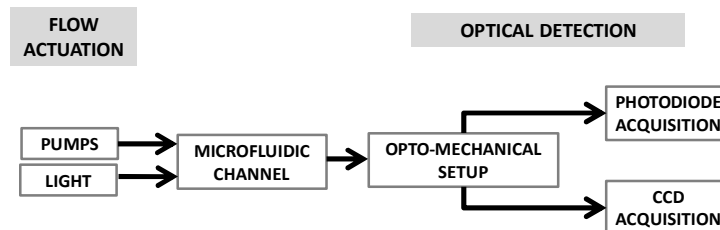

(a)
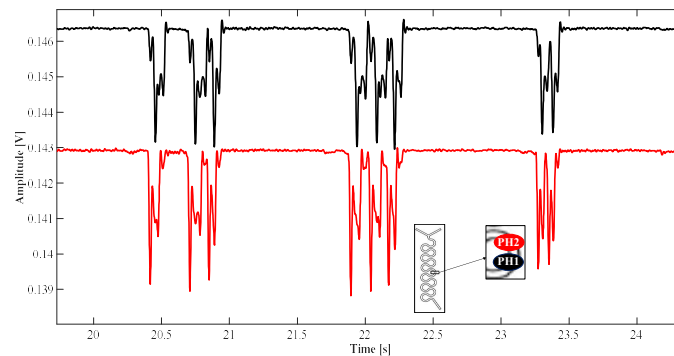
(b)

Figure. 1 (a)The flow chart of the experimental set-up. (b)The trends of the signals acquired by the two photodiodes {*ph1*, *ph2*} for the experiment with an input flow-rate F=0.2 ml/min. In the insert the micro-channel geometry and the positions of the two-photo-diodes.

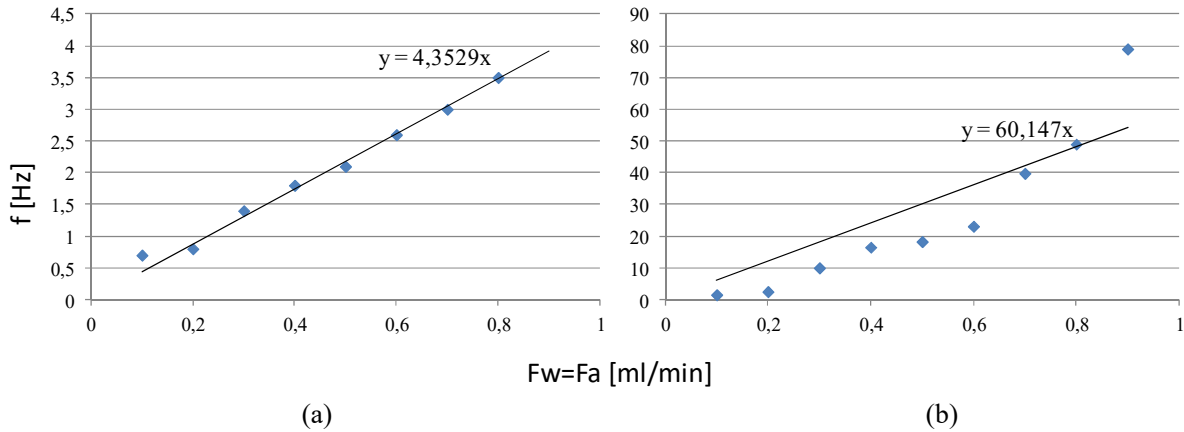## 3. RESULTS

In this works initially the analysis in frequency domain was applied for the *expe-set-1*, the spectrum of the optical signal was computed in time windows of 10 s. For the experiments F∈{0.1, 0.2, 0.3, 0.4, 0.5, 0.6,

A Marie-Curie-ITN
within H2020

Proceedings of the International Symposium on
Thermal Effects in Gas flows In Microscale
October 24-25, 2019 – Ettlingen, Germany

0.7, 0.8} ml/min two frequency peaks were extracted, one in the low frequency range was associated to the longer water-slug passage (*fw*), the second in the high frequency range to shorter air-slug passage (*fa*). For the experiment F=0.9 ml/min only one peak was detected having a fast train of water/air slug at *f*=80 Hz of the same duration. The two peaks are plotted in Fig.3 versus the input flow rate (F=F_a=F_w). The peaks detected in the low frequency are in Fig.3(a), whereas the peaks at high frequency are in Fig.3(b). Fig.3 evidences the ranges of variation of the mean frequency of the water slugs duration passage *fw* $\in [0.5 - 3.5]$ Hz and air frequency *fa* $\in [1 - 48]$ Hz by varying the input flow rate. Therefore a water slug passage can last from $T_w \in [0.3 – 2]$ s and an air slug passage $T_a \in [0.02 -1]$ s. Additionally for F=0.9 ml/min in the air-water train sequence the average duration of the slug passage is f=0.012 s.

(a)

(b)

(c)
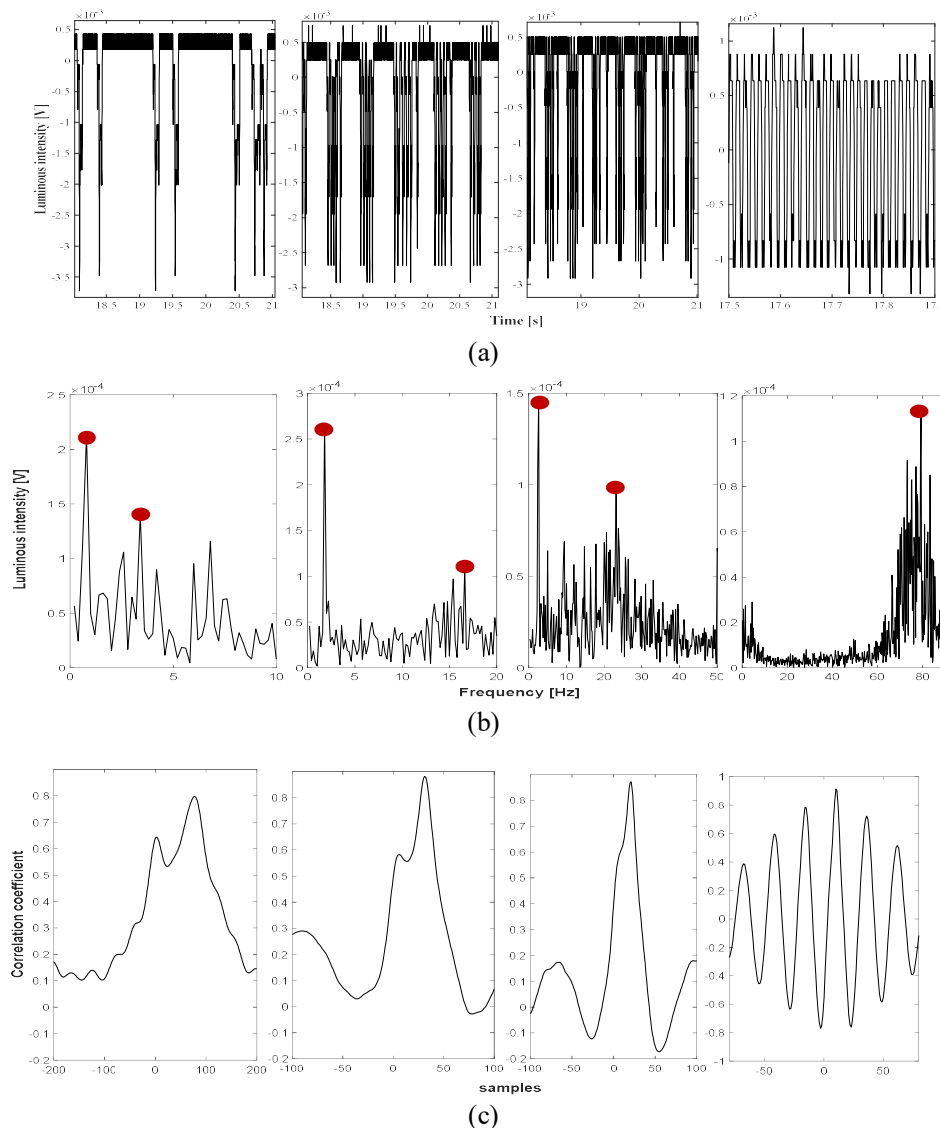
Figure. 2 Dynamics of the slug flows in the *expe-set-1* for the experiments F $\in$ {0.2, 0.4, 0.6, 0.9} ml/min (a) The trends of the raw optical signals acquired varying the input flow rate. It is evident the change of the flow patterns from long water-slugs interlaced by air-slugs one after another (F=0.2 ml/min), to longer water-slugs (F=0.4-0.6 ml/min) followed by a train of smaller air/water passages and finally a train of smaller water/air slugs (F=0.9 ml/min). (b) The spectra of the optical signals for the experiments and the peaks detected (c) The cross-correlation between the signals acquired through the two photodiodes and the peak detected.

4

A Marie-Curie-ITN
within H2020

Proceedings of the International Symposium on
Thermal Effects in Gas flows In Microscale
October 24-25, 2019 – Ettlingen, Germany

Figure. 3 For the *exp-set-1*, the values obtained for the two frequency peaks $\{fw, fa\}$ are in the *y-axis*: (a) the frequency of the water slugs passage (*fw*) and (b) the frequency of the air slugs (*fa*). The input flow-rate is in the *x-axis*. The black line is for the linear interpolation obtained.
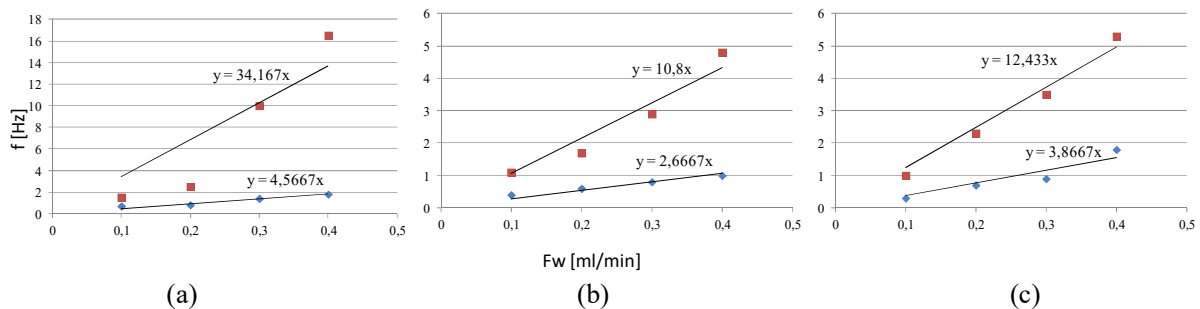
Figure. 4 For the three experimental campaigns {*exp-set-1, exp-set-2, exp-set-3*} the two peaks identified in the spectra $\{fw, fa\}$ were plotted versus the water input flow rate F_w r. In the y-axis of each plot there are the frequency of the slower water slugs' passage (*fw*) in blue dots and the faster frequency of the air slugs' passage (*fa*) in red dots. The black line is for the linear interpolation obtained.

The linear fitting $f(F) = p1 * F + p0 \; (eq.\,(1))$ of the two graphs was computed to establish a mathematical relation between the increase of the frequency of the water/air passage $f \in \{\{fw, fa\}$ varying the input flow rate in the balanced condition {F=Fw=Fa}. The experiment F=0.9 ml/min was excluded in the fitting, being representative of a limit behavior with a different flow pattern. The linear fitting was chosen for a comparison between the {*fw, fa*} plots setting p0=0. The optimal fitting for the *fa* variation vs F is quadratic trend. It is worth to notice that the increase in the air slug frequency is more than one order greater than that of the water slug frequency. To speed up the water it is necessary to move in the condition F=0.9 ml/min.
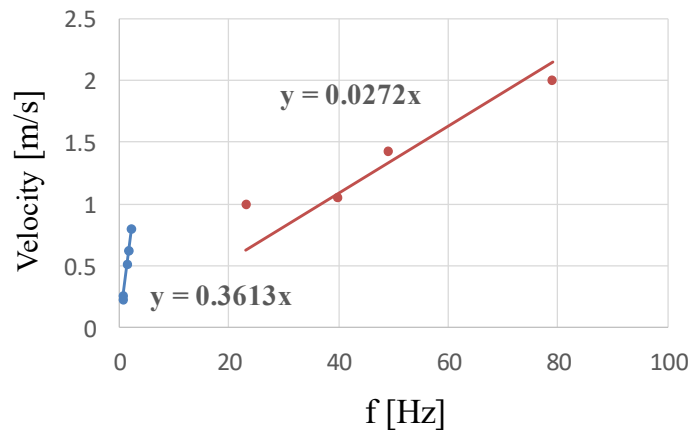
Then, the analysis in the frequency domain was extended to other two experimental campaigns {*expe-set-2, expe-set-3*} having unbalanced input flow rate conditions respectively F_a=1.5* F_w and F_a=2* F_w with $F_w \in \{0.1, 0.2, 0.3, 0.4\}$ ml/min. The flow rates $\{F_w, F_a\}$ are always below the values F=0.9 ml/min, identified as a critical values. The two peaks detected in the spectra were plotted versus the water input flow rate F_w in Figs.4(a) 4(b)- 4(c) respectively for the three experimental campaigns {*exp-set-1, exp-set-2, exp-set-3*}. In the y-axis of each plot there are the frequencies of the water-slugs' passage (*fw*) in blue dots and the frequency of the air-slugs' passage (*fa*) in red dots. Also in this case the linear fitting was performed (eq.1).

In the Figs.4(b)-4(c) for the {*exp-set-2, exp-set-3*} the trends of {*fw, fa*} increase at the increase of the F_w almost linearly and the effect of the greater air input flow rate (Fa) used in the *exp-set-3* can be correlate with the greater values of the slops. A different behavior can be noticed by comparing those with the plots and the

Proceedings of the International Symposium on
Thermal Effects in Gas flows In Microscale
October 24-25, 2019 – Ettlingen, Germany

linear fitting obtained for the *exp-set-1*, reduced for $F_w \in \{0.1, 0.2, 0.3, 0.4\}$ ml/min, as reported in Fig. 4(a). The comparison of the linear interpolation for the *{exp-set-1}* in Fig.3 and Fig.4(a) shows the some results for *fw* and a significant change in *fa*, that can be justified being the linear interpolation not the optimal one, as evident in Fig.4(b) for the red dots.

Generally it is worth to notice that in both {*exp-set-2* , *exp-set-3*}, the increase of {*fw, fa*} are significantly moderate respect to the *{exp-set-1}*. Then having balanced input flow rates (AF=0.5) is possible to have faster slug flow for lower value of {Fa, Fw}. That is also consisted with the results previously obtained [5] showing a increase of the process nonlinearity with no-dominance of one input flow-rate, so an easy process regulation possible in unbalanced conditions.

Finally for the *exp-set-1* the results of the analysis in the frequency domain and time domain were mathematically correlated. The peak of the cross-correlation function value was extracted and the velocity computed, this velocity is related to the two-phase flow with no-distinction for the water and air passage. In the frequency analysis two peaks was detected and associated with the water and air frequency passages. To establish a relation between this two information was assumed that, in all the cases, an increase in the frequency has to lead an increase of the velocity. Following this consideration the frequency of the water-slugs (*fw*) was the most significant to be correlated with the velocity for $F_w \in [0.1,...., 0.5]$ ml/min whereas the frequency of the air-slugs (*fw*) was used in the range $F_w \in [0.6,...., 0.9]$ ml/min, as reported in Fig.6. The nonlinearity of the process and its tendency to move from a flow patter regime to another, as was described in Fig.2, is evidenced by this results and the difference in the two linear interpolations shown in Fig. 6. The blue and the red lines represent the mathematical relation between the velocity and, respectively, the *fw* for $F_w \in [0.1,...., 0.5]$ ml/min and *fa* for $F_w \in [0.6,...., 0.9]$ ml/min.

Fig. 5 Mathematically relation established for the *exp-set-1* between the results of the analysis in the frequency domain and time domain. The values of velocity computed by the dual-slit methodology are reported in the *y-axis* whereas the frequency peak of the water slug *fw* for Fw $\in [0.1,...,0.5]$ ml/min and *fa* for Fw $\in [0.6,...,0.9]$ ml/min are reported in the *x-axis*. The blue and the red lines represent the linear correlation established between the velocity and, respectively, the fw for Fw $\in [0.1,...,0.5]$ ml/min and *fa* for Fw $\in [0.6,...,0.9]$ ml/min.

4. CONCLUSIONS

A challenge in this work was the development of a velocity detection systems, for the slug flow analysis in microchannel, based on optical signals monitoring being non-invasive and suitable for on-chip integration. Being the process highly nonlinear a continuous change in its behavior is expected and the possibility to use low cost simple procedure to track those behaviors represents an important step in the development of microfluidic system-on-chip.

In this works the attention has been focused on two-phase flows obtained by the interaction of immiscible fluids {air and water} in a micro-channels of 320 µm side. Three experimental campaigns {*exp-set-1*, *exp-set-2*, *exp-set-3*} was performed considering balanced (AF=0.5) and unbalanced input flow rates (AF={0.6,

Proceedings of the International Symposium on
Thermal Effects in Gas flows In Microscale
October 24-25, 2019 – Ettlingen, Germany

A Marie-Curie-ITN
within H2020

0.67}). The process was monitored by a photo-diode set-up. Two approaches based on the optical signal's analysis in frequency and time domain were implemented and compared. The first was used to analyze and compare the dominant frequency of the water and air slugs passage obtained in the three experimental conditions. Two dominant frequencies were detected by the spectral analysis a slow one associated to the water passage and a fast one to the air passage. The trends of the increase of {fw, fa} varying the input flow rate were computed experimentally.

The second method based on the dual-slit methodology was used in the *exp-set-1* to establish a mathematical relation between the frequency of the slug passage and the velocity obtained using both photodiode signals *{ph1, ph2}*.

In future works the investigation about the mathematical correlation between the frequency of the slugs passage detected by the spectral analysis and the slugs velocity computed by the dual-slit methodology will be widen and detailed and an real-time procedure for slug velocity detection designed. Additionally a strict control on the pressure at inlet will be realized, being this work focused on the feasibility of using the data analysis to extract slug flows information, independently by the input flow conditions, at this step it was not necessary but it will become for a precise mathematical formulation of the input-output variable relation.

ACKNOWLEDGEMENTS

REFERENCES AND CITATIONS

[1] Anandan P., Gagliano S., Bucolo M. (2015) Computational models in microfluidic bubble logic, *Microfluidics and NanoFluidics*, vol. 18, pp. 305-321.

[2] Bucolo M., Guo J., Intaglietta M. and Coltro W. (2017) Guest Editorial, Special Issue on Microfluidics Engineering for Point-of-Care Diagnostics, *IEEE Trans. on Biomedical Circuits and Systems*, Vol. 11(6), pp. 1488-1499.

[3] Cairone F., Bucolo M. (2016) Data-driven identification of two-phase microfluidic flows, *Mediterranean Conference on Control and Automation,* Athens, Greece.

[4] Cairone F., Gagliano S., Carbone D.C., Recca G., Bucolo M. (2016) Micro-optofluidic switch realized by 3D printing technology, *Microfluidics and Nanofluidics*, vol. 20(4), pp. 61-71.

[5] Cairone F., Gagliano S., Bucolo M. (2016) Experimental study on the slug flow in a serpentine microchannel, *Int. Journal Experimental Thermal and Fluid Science*, Volume 76, pp 34–44.

[6] Cairone F., Anandan P. , Bucolo M. (2018) Nonlinear systems synchronization for modeling two-phase microfluidics flows, *Nonlinear Dynamics* (2018), Vol. 92:75–84.

[7] Gagliano S., Cairone F., Amenta A., and Bucolo M. (2019) A Real Time Feed Forward Control of Slug Flow in Microchannels, *Energies*, 12, 2556.

[8] Kraus T., Gunther A., de Mas N.,. Schmidt M.A, Jensen K.F., (2004) An integrated multiphase flow sensor for microchannels, *Exp. Fluids* 36 819–832.

[9] Kuswandi B., Nuriman J., Huskens W., Verboom W., (2007) Optical sensing systems for microfluidic devices: a review, *Anal. Chim. Acta* 601 (2) 141–155.

[10] Mahvash A., Ross A. (2008) Application of CHMMs to two-phase flow patterns identification, *Engineering Applications of Artificial Intelligence*, vol. 21, pp. 1142-1152.

[11] Mahvash A., Ross A. (2008), Two-phase flow pattern identification using continuous hidden Markov model, *International Journal of Multiphase Flow*, vol. 34, pp. 303-311.

[12] Sapuppo F., Bucolo M., Intaglietta M., Johnson P.C., Fortuna L. and Arena A. (2007) An improved instrument for real-time measurement of blood velocity in microvessels", *IEEE Trans. on Instrumentation and Measurement*, Vol. 56(6), pp.2663:2671.

[13] Sapuppo F., Llobera A., Schembri F., Intaglietta M., Cadarso V.J., Bucolo M., (2010) A polymeric micro-optical interface for flow monitoring in biomicrofluidics, *Biomicrofluidics* 4 (1) 1–13.

*Proceedings of the International Symposium on
Thermal Effects in Gas flows In Microscale
October 24-25, 2019 – Ettlingen, Germany*

[14] Schembri F., F. Sapuppo F. and Bucolo M. (2012) Experimental classification of nonlinear dynamics in microfluidic bubbles flow, *Nonlinear Dynamics* Vol. 67(4), pp. 2807:2819

[16] Seol, D.G., Bhaumik, T., Bergmann, C., Socolofsky, S. A. (2007). Particle Image Velocimetry Measurements of the Mean Flow Characteristics in a Bubble Plume. *Journal of Engineering Mechanics*, 133 (6), pp.665-676.

[17] Qu, J. W., Murai, Y., Yamamoto, F. (2004). Simultaneous PIV/PTV Measurements of Bubble and Particle Phases in Gas-liquid Two-phase Flow Based on Image Separation and Reconstruction, *Journal of Hydrodynamics*, 16(6), pp.756-766.

[18] Worner M. (2012) Numerical modeling of multiphase flows in microfluidics and micro process engineering: a review of methods and applications, *Microfluidics and Nanofluidics*, vol. 12, pp. 841-886.